

The order–disorder phase transition in lipid bilayers mediates a force for assembly of transmembrane proteins

Shachi Katira ^{# *}, Kranthi K. Mandadapu ^{# †}, Suriyanarayanan Vaikuntanathan ^{# ‡}, Berend Smit ^{§ ¶ ||} and David Chandler ^{||}

^{*} Department of Bioengineering, University of California, Berkeley, CA 94720, USA, [†] Chemical Sciences Division, Lawrence Berkeley National Laboratory, Berkeley, CA 94720, USA, [‡] Department of Chemistry, University of Chicago, Chicago, IL, 60637, USA, [§] Department of Chemical and Biomolecular Engineering, University of California, Berkeley, CA 94720, USA, [¶] Institut des Sciences et Ingénierie Chimiques, Valais Ecole Polytechnique Fédérale de Lausanne Rue de l'Industrie 17, Sion CH-1950 Switzerland, and ^{||} Department of Chemistry, University of California, Berkeley, Berkeley, CA 94720 USA

We present a mechanism for a generic and powerful force of assembly and mobility for transmembrane proteins in lipid bilayers. This force is a pre-transition (or pre-wetting) effect for the first-order transition between ordered and disordered phases in the host membrane. Specifically, using large scale molecular simulation, we show that a protein with hydrophobic thickness equal to that of the disordered phase embedded in an ordered bilayer stabilizes a microscopic order–disorder interface, and the line tension of that interface is finite. When two such proteins approach each other, they assemble because assembly reduces the net interfacial free energy. In analogy with the hydrophobic effect, we refer to this phenomenon as the “orderphobic effect.” The effect is mediated by proximity to the order–disorder phase transition and the size and hydrophobic mismatch of the protein. The strength and range of forces arising from the orderphobic effect are significantly larger than those that could arise from membrane elasticity for the membranes we examine.

lipid bilayers, phase transition, hydrophobic mismatch, orderphobe

Abbreviations: DPPC: dipalmitoyl phosphatidylcholine

This paper presents implications of the membrane phase transition we have detailed in the previous paper [1]. The fluid mosaic model [2] and the lipid raft hypothesis [3] have guided intuition on how proteins diffuse in biological membranes—ordered clusters floating in an otherwise disordered fluid membrane [4, 5]. However, recent advances show that the state of membranes containing transmembrane proteins is ordered, even gel-like [6–11]. How then do transmembrane proteins diffuse and assemble within this relatively rigid material? Here, we argue that this question is answered by the fact that a transmembrane protein in an ordered bilayer can induce effects that resemble pre-melting [12, 13]. Specifically, with molecular simulation, we show that within an otherwise ordered membrane phase, mesoscopic disordered domains surround proteins that favor disordered states. We find, importantly, that the boundary of the domains resembles a stable, fluctuating order–disorder interface. The dynamic equilibrium established at the boundary allows the protein and its surrounding domain to diffuse.

Moreover, because the interface has a finite line tension, neighboring proteins can experience a membrane-induced force of adhesion, an attractive force that is distinctly stronger and can act over significantly larger lengths than those that can arise from simple elastic deformations of the membrane [14–18]. This force between transmembrane proteins is analogous to forces of interaction between hydrated hydrophobic objects. In particular, extended hydrophobic surfaces in water can nucleate vapor–liquid-like interfaces. In the presence of such interfaces, hydrophobic objects cluster to reduce the net interfacial free energy. This microscopic pre-transition ef-

fect manifesting the liquid–vapor phase transition can occur at ambient conditions [19–26].

In the transmembrane case, we show here that a protein favoring the disordered phase creates a similar pre-transition effect. In this case it manifests the order–disorder transition of a lipid bilayer. Like the raft hypothesis, therefore, clusters do indeed form, but the mechanism for their assembly and mobility emerge as consequences of order–disorder interfaces in an otherwise ordered phase. We refer to this phenomenon as the “orderphobic effect.”

Transmembrane proteins can disfavor the ordered membrane. To demonstrate the orderphobic effect, we consider the MARTINI model bilayer for dipalmitoyl phosphatidylcholine (DPPC) lipids. We have detailed its order–disorder transition in Ref. [1]. A disordering (i.e., orderphobic) transmembrane protein is one that solvates more favorably in the disordered phase than in the ordered phase. The disordering effect of the protein could be produced by specific side chain structures, though for illustrative purposes, we have considered a simpler mechanism. In particular, we have chosen to focus on the size of the protein’s hydrophobic thickness and the extent to which that thickness matches the thickness of the membrane’s hydrophobic layer [27, 28]. See Fig. 1.

Significance

The clustering of proteins in biological membranes is a controlling factor in processes such as endo- and exo-cytosis, cell signaling, and immunological synapses. Yet physical principles governing this organization are incompletely understood. Here, we address some of this uncertainty by demonstrating a general mechanism for mobility and powerful forces of assembly for transmembrane proteins.

Reserved for Publication Footnotes

[#] These authors contributed equally.

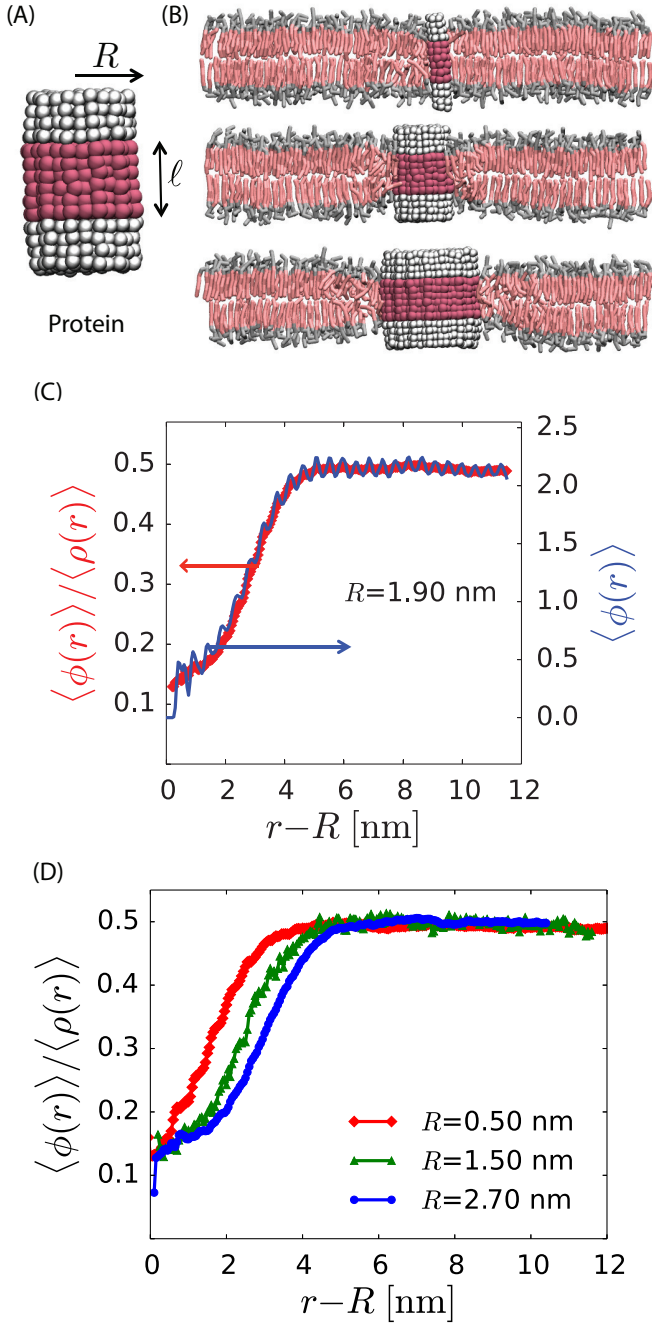


Fig. 1. Model proteins in the bilayer: (A) Idealized cylindrical protein-like solutes with radius R and hydrophobic thickness ℓ (magenta). The hydrophilic caps of the protein are shown in white. (B) Cross sections of lipid bilayers in the ordered phase containing model proteins of three different radii (0.5, 1.5 and 2.7 nm) with a hydrophobic thickness $\ell = 2.3 \text{ nm} \leq \mathcal{L}_d$. (C) The radial variation of the order parameters $\langle \phi(r) \rangle$ (right axis) and $\langle \phi(r) \rangle / \langle \rho(r) \rangle$ (left axis) show disorder in the vicinity of the protein of radius 1.9 nm. (D) Comparison of the radial order parameter variation for three different proteins shows an increase in the extent of the induced disorder region with protein radius. The increase in the spatial extent of the disordered region with the increasing size of the protein is indicative of length scale dependent broadening effects brought about by capillary fluctuations.

The membrane's hydrophobic layer is thicker in the ordered state than in the disordered state. For instance, at zero lateral pressure and 294 K in the model DPPC membrane,

we find that the average thicknesses of the hydrophobic layers in the ordered and disordered states are $\mathcal{L}_o = 3.1 \text{ nm}$ and $\mathcal{L}_d = 2.6 \text{ nm}$, respectively. A transmembrane protein with hydrophobic thickness of size $\ell \approx 2.6 \text{ nm}$ will therefore favor the structure of the disordered phase. If the protein is large enough, it can melt the ordered phase near the protein and result in the formation of an order–disorder interface.

Spatial variation of an order parameter field characterizes spatial extent of pre-melting layer. To distinguish ordered and disordered domains, we consider the order parameter density

$$\phi(\mathbf{r}) = \sum_l \phi_l \delta(\mathbf{r} - \mathbf{r}_l). \quad [1]$$

The notation is that of Ref. [1]: ϕ_l is the Nelson–Halperin rotational invariant that specifies the degree of hexagonal order surrounding the l th tail end particle, \mathbf{r}_l is the position of that particle projected onto the plane of the membrane, and \mathbf{r} is a point in that plane. When coarse-grained over a microscopic length ξ , this order parameter density becomes the field $\bar{\phi}_6(\mathbf{r})$ used in Ref. [1], and below, to identify instantaneous interfaces separating ordered and disordered domains.

In the homogeneous ordered and disordered phases, the average of this field takes on constant values, $\langle \phi(r) \rangle = \phi_o$ and ϕ_d , respectively. At zero lateral pressure and 294 K, the thermodynamic state examined in Figs. 1 (C) and (D), we find $\phi_d = 0.4 \pm 0.02$ and $\phi_o = 2.15 \pm 0.2$. Around the model proteins, the average of this field is a function of $r = |\mathbf{r}|$, $\langle \phi(r) \rangle$ (right axis of Fig. 1C). It exhibits oscillations manifesting the atomistic granularity of the system. Dividing by the mean density, $\langle \rho(r) \rangle = \langle \sum_l \delta(\mathbf{r} - \mathbf{r}_l) \rangle$, removes these oscillations. The ratio, $\langle \phi(r) \rangle / \langle \rho(r) \rangle$ has values 0.15 and 0.45 in the ordered and disordered phases respectively. A profile of this quantity in the vicinity of the protein is depicted in Fig. 1C (left axis). The profile changes sigmoidally, connecting its values of 0.15 and 0.45 in the disordered and ordered phases, respectively. The shape of the profile suggests the formation of an order–disorder interface. Further, the increase in the spatial extent of the disordered region with the increasing size of the protein Fig. 1D is indicative of length scale dependent broadening effects brought about by capillary fluctuations.

An orderphobic protein nucleates a fluctuating order–disorder interface. Fig. 2B shows a configuration of the instantaneous interface that forms around an orderphobic protein. The interface is identified as in Ref. [1]. Specifically, it is the contour \mathbf{s} satisfying $\bar{\phi}(\mathbf{s}) = (\phi_o + \phi_d)/2$. It is continuous and fluctuating interface that remains intact throughout our simulations. A video of its dynamics is provided at <https://goo.gl/NBQJJP9>.

The mean interface is a circle of radius \mathcal{R}_0 . Fourier analysis of fluctuations about that circle yields a spectrum of components. To the extent that these fluctuations obey statistics of capillary wave theory for circular interface, the mean-square fluctuation for the k th component is $\langle |\delta \mathcal{R}_k|^2 \rangle = k_B T / 2\pi \gamma k^2 \mathcal{R}_0$, where $k = m/\mathcal{R}_0$ and $m = \pm 1, \pm 2, \dots$, and γ is the order–disorder line tension. Here, the discrete values of k reflect periodic boundary conditions going full circle around the model protein. In Ref. [1], values of k are spaced reflecting periodic boundary conditions for the entire plane of the membrane. There, we found $\gamma = 11.5 \text{ pN}$ for the free interface separating coexisting ordered and disordered phases. In Fig. 2C, we use this line tension with the capillary theory expression [29] and the spectrum of a free order–disorder interface at coexistence to compare with the spectrum found in our simulations. The agreement between the theory, free

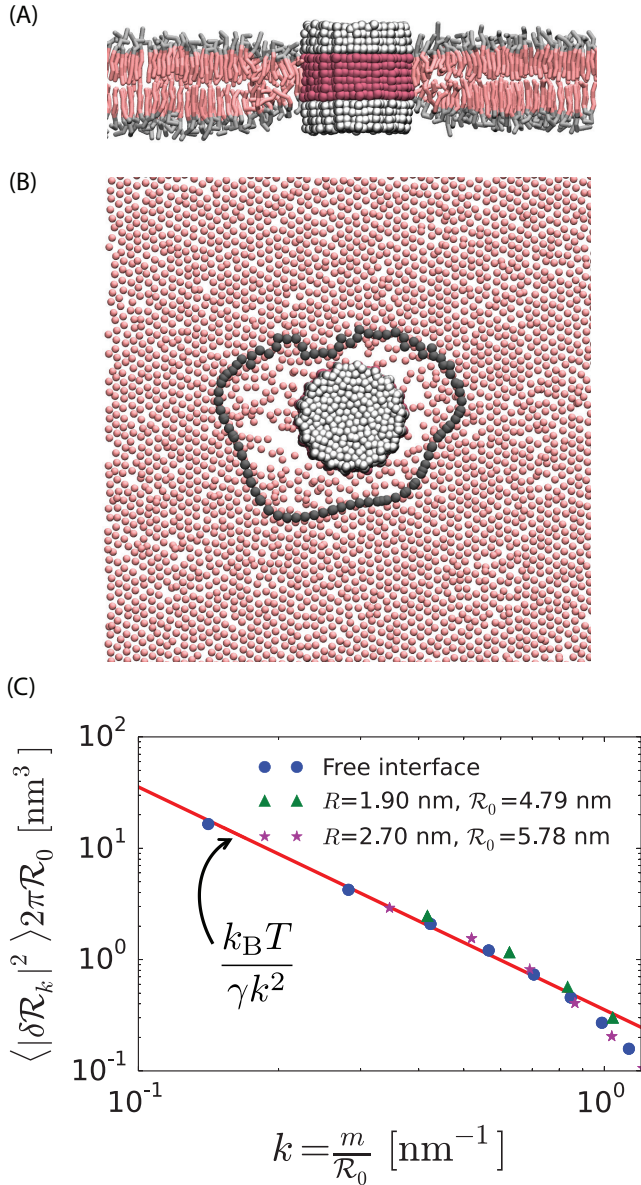


Fig. 2. Soft order–disorder interface: (A) Arrangement of lipids in the vicinity of the protein of radius 1.9 nm. (B) Arrangement of the tail end particles of the top monolayer. Far away from the protein, the tail end particles show hexagonal-like packing and are in the ordered state. Proximal to the protein, it can be seen that the tail end particles are randomly arranged, and resemble the disordered phase [1]. The line connected by the black points denotes the instantaneous order–disorder interface. As in Ref. [1], the empty regions in the disordered domain are not literally devoid of particles. Only tail-end particles from one of the two monolayers are rendered. The empty regions are in fact filled with other particles, either tail-end particles from the other of the two monolayers or from non-tail-end positions on the chains. (C) The fluctuations in the radius of the order–disorder interface are consistent with the fluctuations of a free order–disorder interface at coexistence [1]. R_0 is the mean radius of the order–disorder interface surrounding a model protein of radius R .

interface and the protein-induced interface is good, and it improves as the radius of the orderphobic protein increases and the wave vector k decreases. This agreement indicates that the orderphobic protein does indeed nucleate an interface as a manifestation of the order–disorder transition.

The deviations of the fluctuations of the free interface from capillary wave theory occur for $k \gtrsim 0.85 \text{ nm}^{-1}$, corresponding

to wavelengths $2\pi/k \lesssim 7.4 \text{ nm}$, and a mean interface radius $R_0 \lesssim 1.2 \text{ nm}$. Indeed, Fig. 1 suggests that even a small protein of radius 0.5 nm, which supports an interface of radius $R_0 \approx 1.2 \text{ nm}$ is sufficient to induce an order–disorder interface with fluctuations consistent with capillary theory.

The orderphobic effect generates a force for protein assembly.

To demonstrate the existence of a force for assembly, we begin with two orderphobic proteins of diameter 1.5 nm initially separated by a distance of 14 nm. Each induces a disordered region in its vicinity, with soft interfaces separating the ordered and disordered regions. See Fig. 3A. The free energy of the separated state is approximately $\gamma(P_1 + P_2)$, where P_i is the perimeter of the order–disorder interface around protein i . On average, $\langle P_i \rangle = 2\pi R_0$. After a few hundred nanoseconds, a fluctuation occurs where the two interfaces combine. While the single large interface remains intact, the finite tension of the interface pulls the two proteins together. Eventually, the tension pulls the two proteins together with a final perimeter, P_f , that is typically much smaller than $P_1 + P_2$. A video of its dynamics is provided at <https://goo.gl/HXS0j7>.

With the net interface remaining intact, the assembly process occurs on the time scale of microseconds. This time is required for the proteins to push away lipids that lie in the path of the assembling proteins. The net driving force for assembly is large compared to thermal energies. For example, with model orderphobic protein radius of 1.5 nm, we find $\gamma(\langle P_f \rangle - 2\langle P_1 \rangle) \approx -30 k_B T$. Further, $2R_0 \approx 10$ to 30 nm is the typical range over which this force acts. In comparison, given the elastic moduli of the membranes we consider, elastic responses will generate attractive forces between transmembrane proteins that are much smaller in strength and range, typically $-5 k_B T$ and 1 nm, respectively [18,30].

As in the hydrophobic effect [19], the strength and range of the orderphobic force leverages the power of a phase transition, depending in this case on the ability of the orderphobic protein to induce a disordered layer in its vicinity. This ability depends upon the proximity to the membrane’s phase transition, and, for the simple protein models considered in this paper, it depends upon the protein’s radius and hydrophobic mismatch with the membrane. The spatial extent of the disordered region increases with proximity to phase coexistence as shown in Fig. 4A. Furthermore, Fig. 4B shows that the strength of the effect is maximal for a hydrophobic thickness equal to that of the disordered phase, and it decreases as the hydrophobic thickness approaches that of the ordered phase. In the case of zero mismatch, i.e., $\ell = L_o$, the value of the order parameter in the vicinity of the protein is consistent with that of a pure bilayer in the ordered state. Therefore, the model proteins with zero mismatch, do not induce a disordered region, and the orderphobic effect vanishes. See Figs. 4B and 4D.

Orderphobic proteins increase mobility in the ordered phase.

Along with generating a powerful force of assembly, the orderphobic effect also creates excess mobility in the ordered phase. This excess is apparent in the assembly trajectory illustrated in Fig. 3. Further information on this phenomenon is provided in Fig. 5, where we compare mean-square displacements of lipids in the ordered phase, the disordered phase and the disordered region surrounding a model orderphobic protein.

Note that the center of mass of the membrane fluctuates in time. These fluctuations affect the absolute positions of lipid molecules, but they are irrelevant to the issue of lipid mobility. Therefore, the mean-square displacements considered in Fig. 5 are for tail-end particle positions *relative* to the instantaneous position of the membrane’s center of mass. That is to

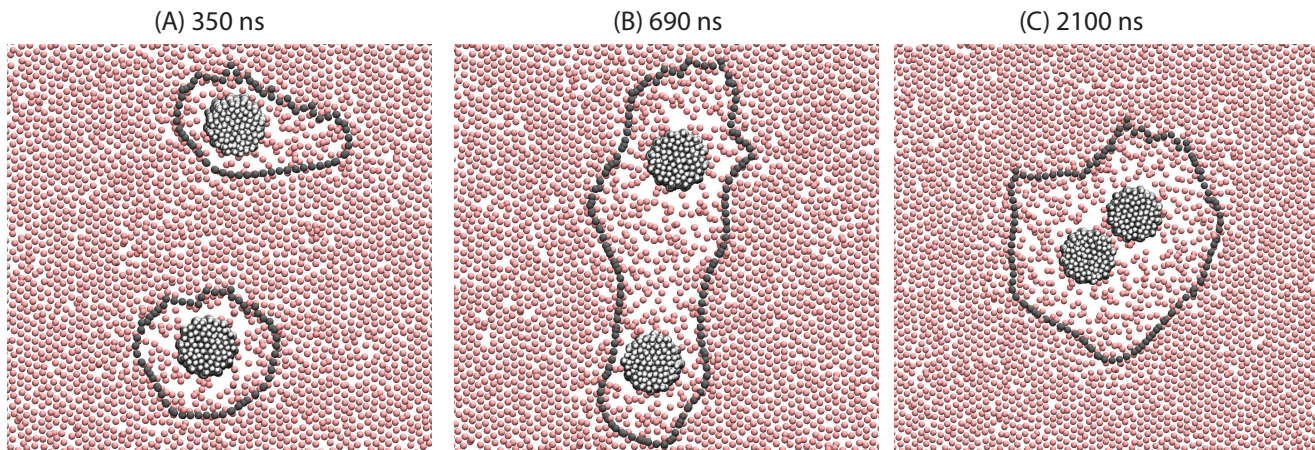


Fig. 3. Demonstration of the orderphobic force: Two proteins separated by a center-to-center distance of 14 nm are simulated at 309 K. Snapshots at various times reveal the process of assembly in which the two order–disorder interfaces merge into a single interface.

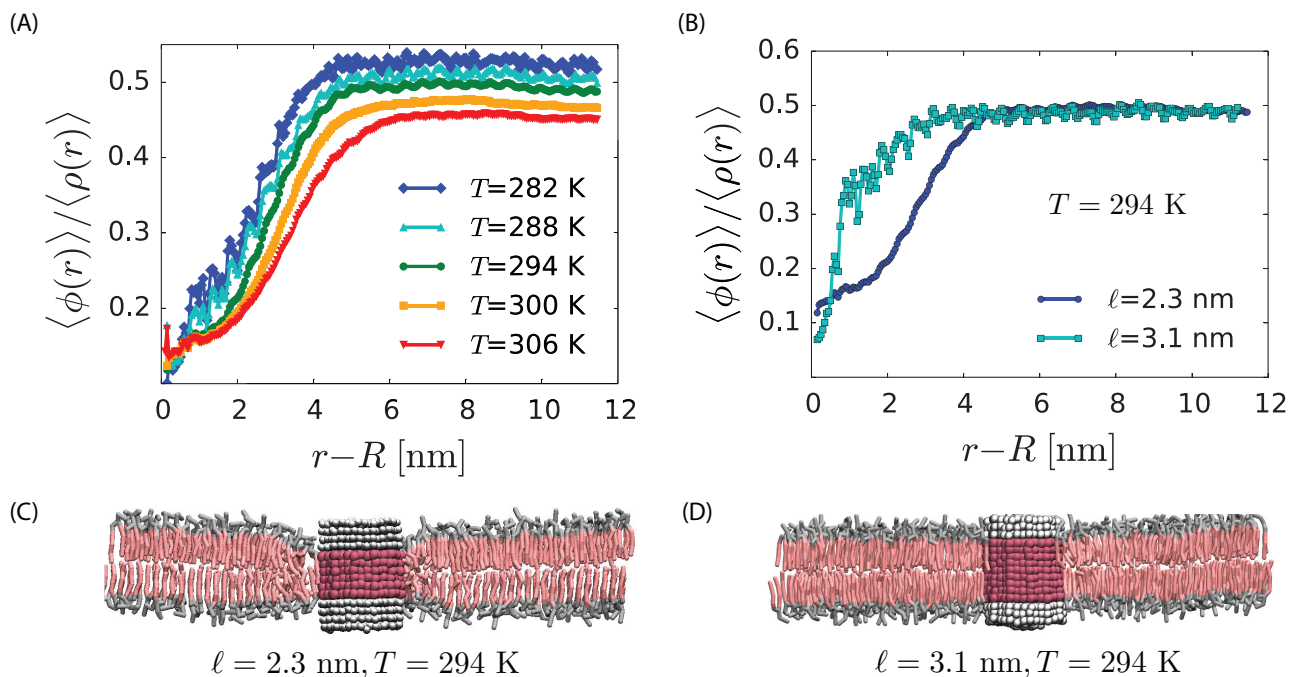


Fig. 4. Strength of the orderphobic force: (A) Radial variation of the order parameter showing the extent of the disordered region as a function of temperature, for a protein of radius 1.9 nm and hydrophobic thickness 2.3 nm. The extent of the disordered region increases as the melting temperature is approached, at zero surface tension. (B) Comparison of the radial variation of the order parameter for different hydrophobic mismatches. Proteins with no mismatch do not create any disordered region. (C) Arrangement of lipids around a protein with negative mismatch. (D) Arrangement of lipids around a protein with zero mismatch.

say, for $\langle |\bar{\mathbf{r}}_l(t) - \bar{\mathbf{r}}_l(0)|^2 \rangle$, where $\bar{\mathbf{r}}_l(t)$ is the position at time t of the l th tail-end particle less that of the membrane’s center of mass. On the scale of Fig. 5, lipid mobility in the ordered phase is virtually negligible compared to that in the disordered phase. Yet the figure shows that lipid mobility near an orderphobic protein in the ordered phase is faster than that of the ordered phase. This finding is amenable to experimental tests. Moreover, in view of Fig. 3, it provides an explanation for how protein mobility and reorganization can be relatively facile in the so-called “gel” phases of membranes.

Implications of the orderphobic effect and related phenomena in biological membranes. Biological membranes are far more complicated than the models considered in this paper. Part of the complexity is associated with multiple components, which can be studied outside of biological contexts. For example, we

anticipate that the orderphobic effect will be useful in understanding the phase behavior that results from mixing cholesterol with pure or multicomponent lipid bilayers [31–34]. In this case, cholesterol with a small hydrophilic head and short hydrophobic tail has the propensity to induce disorder in the ordered phase [33].

Further, there is a dual to the orderphobic effect: A trans-membrane protein in the disordered phase that favors the ordered phase can nucleate an ordered region and order–disorder interface. For example, one of our model proteins with a positive mismatch ($\ell = \mathcal{L}_o$) would induce order in its vicinity. Interfaces separating the ordered and disordered regions will again provide a force for assembly. This case corresponds to the situation of lipid rafts [3], which consists of ordered domains floating in otherwise disordered membranes.

Finally, we speculate that the orderphobic effect plays important roles in membrane fusion and cell signaling [35–37]. In the case of fusion, it would appear that one important role is to promote fluctuations in an otherwise stable membrane. Otherwise, it is difficult to conceive of a mechanism by which thermal agitation would be sufficient to destabilize microscopic sections of membranes. Such destabilization seems necessary for initiating and facilitating membrane fusion. Granted, many proteins are involved in such processes [35, 38, 39], but it may not be a coincidence that the hydrophobic thicknesses of SNARE proteins are 25% smaller than that of the ordered membrane states [40, 41].

Materials and Methods

Model. We use molecular simulation methods for studying the orderphobic effect. To model the interaction between lipids and their interaction with proteins, we use the MARTINI coarse-grained force field [42] as in [1]. The proteins in our system are idealized proteins, which contain a hydrophobic core with hydrophilic caps. The hydrophobic core is constructed using the same coarse-grained beads as the lipid tails (particle C1 in the MARTINI topology [42]). Similarly, the hydrophilic caps are constructed using the first bead of the DPPC head group (Q0, in the MARTINI topology). The protein beads also have bonded interactions where the bond length is 0.45 nm and the bond angle is set to 180° . The associated harmonic force constants for the bond lengths and angles are $1250 \text{ kJmol}^{-1} \text{ nm}^{-2}$ and $25 \text{ kJmol}^{-1} \text{ rad}^{-2}$. Based on the hydrophobic mismatch with the bilayers, the proteins are classified into three categories: (i) positive mismatch ($\ell > \mathcal{L}_o$) (ii) negative mismatch ($\ell \leq \mathcal{L}_d$) and (iii) no mismatch ($\ell \approx \mathcal{L}_o$). To create different mismatches, we alter the number of beads in the protein core. We note that these idealized proteins do not contain charges.

Molecular Dynamics Simulations. We perform simulations using the GROMACS molecular dynamics package [43] as in [1]. Proteins are embedded in the equilibrated bilayer at 279 K. The resulting system is then heated to the required temperature and equilibrated for another 1.2 μs . All the subsequent averages are performed using 10 independent trajectories each 600 ns long. The assembly of proteins is also performed using the same DPPC bilayer system with 3200 lipids and 50000 water beads. In this case, two proteins are inserted in this bilayer with centers at a distance of 14 nm and the simulation is carried out at 309 K.

1. Katira, S, Mandadapu, K. K, Vaikuntanathan, S, Smit, B & Chandler, D. (2015) The order–disorder transition in model lipid bilayers is a first-order hexatic to liquid phase transition. arXiv:1506.04310.
2. Singer, S. J & Nicholson, G. L. (1972) The fluid-mosaic model of the structure of cell membranes. *Science* 175:720–731.
3. Simons, K & Ikonen, E. (1997) Functional rafts in cell membranes. *Nature* 387:569–572.
4. Simons, K & Toomre, D. (2000) Lipid rafts and signal transduction *Nature Reviews Molecular Cell Biology* 1:31–39.
5. Lingwood, D & Simons, K. (2010) Lipid rafts as a membrane-organizing principle. *Science* 327:46–50.
6. Nishimura, S. Y, Vrljic, M, Klein, L. O, McConnell, H. M & Moerner, W. E. (2006) Cholesterol depletion induces solid-like regions in the plasma membrane. *Biophysical Journal* 90:927–938.
7. Polozov, I. V, Bezrukov, L, Gawrisch, K & Zimmerberg, J. (2008) Progressive ordering with decreasing temperature of the phospholipids of influenza virus. *Nature Chemical Biology* 4:248–55.
8. Swamy, M. J, Ciani, L, Ge, M, Smith, A. K, Holowka, D, Baird, B & Freed, J. H. (2006) Coexisting domains in the plasma membranes of live cells characterized by spin-label ESR spectroscopy. *Biophysical Journal* 90:4452–4465.
9. Munro, S. (2003) Lipid rafts: elusive or illusive? *Cell* 115:377–388.
10. Thewalt, J. L & Bloom, M. (1992) Phosphatidylcholine cholesterol phase diagrams. *Biophysical Journal* 63:1176–1181.
11. Owen, D. M, Williamson, D. J, Magenau, A & Gaus, K. (2012) Sub-resolution lipid domains exist in the plasma membrane and regulate protein diffusion and distribution. *Nature Communications* 3:1–7:1256.
12. Lipowsky, R. (1982) Critical surface phenomena at first-order bulk transitions. *Physical Review Letters* 49:1575.
13. Lipowsky, R. (1984) Surface-induced order and disorder: Critical phenomena at first-order phase transitions. *Journal of Applied Physics* 55:2485–2490.
14. Dan, N, Pincus, P & Safran, S. A. (1993) Membrane-induced interactions between inclusions. *Langmuir* 9:2768–2771.

ACKNOWLEDGMENTS. S. V. acknowledges support from the University of Chicago. S. V. acknowledges support for the initial part of the work from Director, Office of Science, Office of Basic Energy Sciences, Materials Sciences, and Engineering Division, of the U.S. Department of Energy under contract No. DE-AC02-05CH11231. S. K. and B. S. is supported by the Chemical Sciences, Geosciences and Biosciences Division, Office of Basic Energy Sciences, Office of Science of the U.S. Department of Energy, FWP number SISGRKN. K.K.M. and D. C. are supported by the Chemical Sciences Division at Lawrence Berkeley National Laboratory under Contract No. DE-AC02-05CH11231 with the U.S. Department of Energy. This research used resources of the National Energy Research Scientific Computing Center, a DOE Office of Science User Facility supported by the Office of Science of the U.S. Department of Energy under Contract No. DE-AC02-05CH11231. The authors also acknowledge support from Midway-RCC computing cluster at University of Chicago.

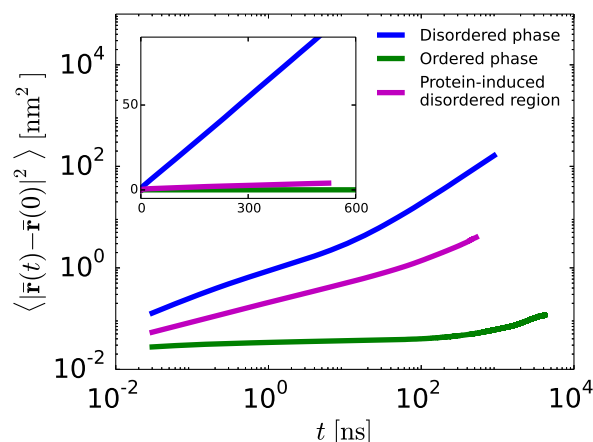


Fig. 5. Mean squared displacements of the lipids in the protein induced disordered domain, bulk ordered and disordered phases in the log and linear (Inset) scales. The data shows that protein induced disordered region has higher mobility than that of the ordered phase.

15. Goulian, M, Bruinsma, R & Pincus, P. (1993) Long-range forces in heterogeneous fluid membranes. *Europhysics Letters* 22:145–150.
16. Phillips, R, Ursell, T, Wiggins, P & Sens, P. (2009) Emerging roles for lipids in shaping membrane-protein function. *Nature* 459:379–385.
17. Kim, K. S, Neu, J & Oster, G. (1998) Curvature-mediated interactions between membrane proteins. *Biophysical Journal* 75:2274–2291.
18. Haselwandter, C. A & Phillips, R. (2013) Directional interactions and cooperatively between mechanosensitive membrane proteins. *Europhysics Letters* 101:68001–1–6.
19. Chandler, D. (2005) Interfaces and the driving force of hydrophobic assembly. *Nature* 437:640–647.
20. Lum, K, Chandler, D & Weeks, J. D. (1999) Hydrophobicity at small and large length scales. *The Journal of Physical Chemistry B* 103:4570–4577.
21. Willard, A. P & Chandler, D. (2008) The role of solvent fluctuations in hydrophobic assembly. *The Journal of Physical Chemistry B* 112:6187–6192.
22. Stillinger, F. H. (1973) Structure in aqueous solutions of nonpolar solutes from the standpoint of scaled-particle theory. *Journal of Solution Chemistry* 2:141–158.
23. ten Wolde, P. R & Chandler, D. (2002) Drying-induced hydrophobic polymer collapse. *Proceedings of National Academy of Sciences* 99:6539–6543.
24. Mittal, J & Hummer, G. (2008) Static and dynamic correlations in water at hydrophobic interfaces. *Proceedings of National Academy of Sciences* 105:20130–20135.
25. Patel, A. J, Varilly, P, Jamadagni, S. N, Acharya, H, Garde, S & Chandler, D. (2011) Extended surfaces modulate hydrophobic interactions of neighboring solutes. *Proceedings of National Academy of Sciences* 108:17678–17683.
26. Patel, A. J, Varilly, P, Jamadagni, S. N, Hagan, M. F, Chandler, D & Garde, S. (2012) Sitting at the edge: How biomolecules use hydrophobicity to tune their interactions and function. *The Journal of Physical Chemistry B* 116:2498–2503.
27. Killian, J. A. (1998) Hydrophobic mismatch between proteins and lipids in membranes. *Biochimica et Biophysica Acta (BBA)* 1376:401–416.
28. Sharpe, H. J, Stevens, T & Munro, S. (2010) A comprehensive analysis of transmembrane domains reveals organelle-specific properties. *Cell* 142:158–169.
29. Rowlinson, J. S & Widom, B. (1982) *Molecular theory of capillarity*. (Clarendon Press: Oxford).

30. De Meyer, F. J. -M, Venturoli, M & Smit, B. (2008) Molecular simulations of lipid-mediated protein-protein interactions. *Biophysical Journal* 95:1851–1865.
31. Ipsen, J. H, Karlstrom, G, Mouritsen, O. G, Wennerstrom, H & Zuckermann, M. J. (1987) Phase equilibria in the phosphatidylcholine-cholesterol system. *Biochimica et Biophysica Acta (BBA)* 905:162–172.
32. Risselada, H. J & Marrink, S. J. (2008) The molecular face of lipid rafts in model membranes. *Proceedings of National Academy of Sciences* 105:17367–17372.
33. Sodd, A. J, Sandar, M. L, Gawrisch, K, Pastor, R. W & Lyman, E. (2014) The molecular structure of the liquid-ordered phase of lipid bilayers. *Journal of American Chemical Society* 136:725–732.
34. Radhakrishnan, A & McConnell, H. M. (2005) Condensed complexes in vesicles containing cholesterol and phospholipids. *Proceedings of National Academy of Sciences* 102:12662–12666.
35. Fratti, R. A, Jun, Y, Merz, A. J, Margolis, N & Wickner, W. (2004) Interdependent assembly of specific regulatory lipids and membrane fusion proteins into the vertex ring domain of docked vacuoles. *The Journal of cell biology* 167:1087–1098.
36. Zick, M, Stroupe, C, Orr, A, Douville, D & Wickner, W. T. (2014) Membranes linked by trans-SNARE complexes require lipids prone to non-bilayer structure for progression to fusion. *Elife* 3:e01879.
37. James, J. R & Vale, R. D. (2012) Biophysical mechanism of T-cell receptor triggering in a reconstituted system. *Nature* 487:64–69.
38. Fasshauer, D, Bryan Sutton, R, Brunger, A. T & Jahn, R. (1998) Conserved structural features of the synaptic fusion complex: SNARE proteins reclassified as Q- and R-SNAREs. *Proceedings of National Academy of Sciences* 95:15781–15786.
39. Wickner, W & Schekman, R. (2008) Membrane fusion. *Nature Structural & Molecular Biology* 15:658–664.
40. Milovanovic, D et. al. (2015) Hydrophobic mismatch sorts SNARE proteins into distinct membrane domains. *Nature Communications* 6:5894.
41. Stein, A, Weber, G, Wahl, M. C & Jahn, R. (2015) Helical extension of the neuronal SNARE complex into the membrane. *Nature* 460:525–528.
42. Marrink, S. J, Risselada, H. J, Yefimov, S. Y, Tieleman, D. P & de Vries, A. H. (2007) The MARTINI force field: Coarse grained model for bimolecular simulations. *The Journal of Physical Chemistry B* 111:7812–7824.
43. Pronk, S, Pail, S, Schulz, R, Larsson, P, Bjelkmar, P, Apostolov, R, Shirts, M. R, Smith, J. C, Kasson, P. M, van der Spoel, D, Hess, B & Lindahl, E. (2013) GRO-MACS 4.5: A high-throughput and highly parallel open source molecular simulation toolkit. *Bioinformatics* 29:845–854.